

# SELF-MODULATION OF A RELATIVISTIC ELECTRON BEAM IN A WIGGLER\*

J. P. MacArthur,<sup>†</sup> J. Duris, Z. Zhang, Z. Huang, A. Marinelli  
 SLAC National Accelerator Laboratory, Menlo Park, USA

## Abstract

Users at x-ray free-electron laser (FEL) facilities have shown strong interest in using single spike, coherent x-ray pulses to probe attosecond dynamics in atoms and molecules. Sub-femtosecond soft x-ray pulses may be obtained from an electron beam that has been modulated in a wiggler resonant with an external laser, the enhanced-SASE technique. We discuss a new way to produce this energy modulation, wherein the external laser is replaced by coherent radiation from the current spike on the tail of the electron beam. We calculate the modulation expected in a wiggler from both a single frequency perspective and a coherent synchrotron radiation (CSR) perspective.

## INTRODUCTION

An ongoing project to produce sub-femtosecond x-ray pulses for users at the Linac Coherent Light Source (LCLS) was designed to implement the enhanced self-amplified spontaneous emission (ESASE) technique [1]. In ESASE, an external seed laser resonant to a wiggler is co-propagated with an electron beam that receives a sinusoidal energy modulation. This energy modulation can be converted into a series of density spikes with the soft x-ray seeding chicane already integrated into the LCLS undulator line. A single density spike can be selected to lase with a number of methods, including the emittance slotted spoiler [2] and the fresh-slice technique [3, 4].

The sinusoidal energy modulation produced by the external laser in the wiggler must be large enough for the chicane to fully compress the chirped portion of the electron beam. The soft x-ray self seeding chicane at LCLS has a maximum  $R_{56}$  of 0.5 mm, meaning the energy modulation amplitude must be at least a few MeV in order to fully compress a beam modulated at a few micron wavelength.

It is also important to suppress any additional energy modulation from coherent synchrotron radiation produced during bunch compression upstream of the wiggler. This is typically accomplished by increasing the energy spread of the beam with a laser heater [5] and collimating the short current spikes on the head and tail of the electron beam in the dispersive portion of a bunch compressor [2].

If the tail is not collimated away, it is short enough to emit coherently in the wiggler at the frequency resonant with the wiggler. This coherent wiggler radiation is powerful enough to replace the external laser and modulate the electron beam. An example of a self-modulated electron beam is shown in Fig. 1.

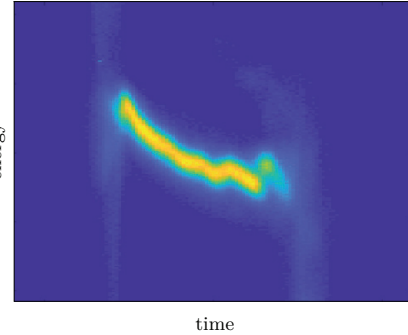


Figure 1: An image of the transverse phase space of the LCLS electron beam following self-modulation in a six period wiggler. The bunch tail is on the right. Two or three periods of self modulation are evident next to the tail of the beam. The modulation period is approximately 1 fs.

In this paper we endeavor to understand the self-modulation displayed in Fig. 1. We first approach the problem by solving the Maxwell equation for the diffracting field produced by a pancake beam, and allowing this field to modulate the electron beam. We then compare this single frequency approach with the energy modulation expected from an exact 1D CSR model of energy modulation in a wiggler.

## SINGLE FREQUENCY MODEL

The paraxial equation for the field envelope  $E_\nu$  resulting from an electron beam composed of  $N_e$  electrons at transverse position  $\mathbf{x}_j$  is [6]

$$\left[ \frac{\partial}{\partial z} + i\Delta\nu k_u - i\frac{\nabla^2}{2k} \right] E_\nu(\mathbf{x}; z) = -\frac{\kappa_1 k}{2\pi} \sum_{j=1}^{N_e} e^{-i\nu\theta_j} \delta(\mathbf{x} - \mathbf{x}_j), \quad (1)$$

where  $z$  is the propagation distance in the lab frame,  $\nu = \Delta\nu + 1 = k/k_1$  is the frequency relative to the resonant frequency  $k_1$ ,  $k_u$  is the wiggler wavenumber,  $\kappa_1 = eK[JJ]/4\epsilon_0\gamma$  is a coupling constant, and  $\theta$  is the ponderomotive phase.

Unfortunately, Eq. (1) relies on two assumptions that are of questionable applicability for our problem. The first is the slowly varying amplitude approximation, which is valid when  $E_\nu$  varies slowly over a length  $2\pi/k$ . This is typically satisfied when the number of wiggler periods is large,

$$N_u \gg 1. \quad (2)$$

Our wiggler has 6 periods. However, the portion of the beam that receives the largest modulation is less than one period

\* Work supported by DOE contract DE-AC02-76SF00515.

<sup>†</sup> jmacart@slac.stanford.edu

from the source. The other assumption appropriate for FEL physics calculations but of questionable applicability here is that the non-resonant charge density source term is much smaller than the current source term. This approximation is appropriate for radiation forming at angles  $|\phi| \ll K/\gamma$ .

In FEL calculations, we are interested in radiation forming in the central cone, where  $\gamma|\phi| \lesssim 1/\sqrt{N_u}$ . Fortunately in our case  $K \approx 40$ . However, in the case of a wiggler with  $K \gg 1$ , the radiation field is concentrated in a cone much narrower than the angular motion of the electrons. Thus, the on-axis field modulating the beam near the source must have a significant angular component, perhaps approaching the maximum angular deviation of the beam,  $K/\gamma$ .

In this section we ignore these concerns, and proceed to solve Eq. (1) in order to build intuition.

The current spike on the tail of the beam can be shorter than the resonant wavelength of our wiggler, so we assume for the moment that all  $N_e$  electrons in the tail are emitting coherently,  $\theta_j(z) = 0$ . Eq. (1) is readily solved in the spatial frequency domain, where

$$\tilde{E}_v(\phi) = \frac{1}{\lambda^2} \int d\mathbf{x} e^{-ik\mathbf{x}\cdot\phi} E_v(\mathbf{x}). \quad (3)$$

Transforming both sides of Eq. (1) and assuming the electron beam has a normalized transverse distribution  $f(\mathbf{x})$ , the electric field in the frequency domain can be directly computed from the Maxwell equation in the frequency domain,

$$\left[ \frac{\partial}{\partial z} + i \left( \Delta v k_u + \frac{k}{2} \phi^2 \right) \right] \tilde{E}_v = -\frac{\kappa_1 N_e}{\lambda^3} \int d\mathbf{x} e^{-ik\mathbf{x}\cdot\phi} f(\mathbf{x}). \quad (4)$$

After choosing a transverse distribution  $f(\mathbf{x})$ , the electric field may be inserted into the pendulum equation [6] for the field-induced energy modulation  $\Delta\gamma/\gamma = \eta$ ,

$$\frac{d\eta}{dz} = \chi_1 \int dv e^{iv\theta} \int d\phi e^{ik\phi\cdot\mathbf{x}} \tilde{E}_v + \text{c.c.}, \quad (5)$$

where  $\chi_1 = eK[\text{JJ}]/2\gamma^2 m c^2$ . Eq. (5) is a wiggler averaged expression, meaning non-resonant terms that vary rapidly over a wiggler period have been dropped. If the source term is a two dimensional Gaussian,

$$f(\mathbf{x}) = \frac{e^{-\frac{x^2}{2\sigma_x^2} - \frac{y^2}{2\sigma_y^2}}}{2\pi\sigma_x\sigma_y}, \quad (6)$$

there is an algebraic expression for  $\tilde{E}_v$ . Applying Eq. (5) and integrating with respect to  $z$ , the resulting energy modulation is

$$\eta(\mathbf{x}, \theta) = -a \frac{\exp \left[ i\theta - \frac{x^2}{2(\hat{\sigma}_x^2 + i\theta)} - \frac{y^2}{2(\hat{\sigma}_y^2 + i\theta)} \right]}{\sqrt{(i\theta + \hat{\sigma}_x^2)(i\theta + \hat{\sigma}_y^2)}} (k_u z - \theta) + \text{c.c.} \quad (7)$$

when  $0 \leq \theta \leq k_u z$ , and  $\eta(\mathbf{x}, \theta) = 0$  otherwise. The amplitude  $a = k N_e r_e [\text{JJ}]^2 / \gamma$  is most compactly written in terms

of the classical electron radius  $r_e$ ,  $\hat{x} = x\sqrt{k k_u}$ ,  $\hat{y} = y\sqrt{k k_u}$ ,  $\hat{\sigma}_x = \sigma_x\sqrt{k k_u}$ , and  $\hat{\sigma}_y = \sigma_y\sqrt{k k_u}$ .

The  $(k_u z - \theta)$  dependence of Eq. (7) is a result of finite drift in the wiggler. After a distance  $z$ , radiation from a pancake source at  $\theta = 0$  created at  $z = 0$  has only drifted forward by  $k_u z / 2\pi$  wavelengths. Electrons beyond that range have received no radiation, and are therefore not modulated. Test electrons behind the source receive no radiation, and therefore no modulation.

If the source pancake beam generating the modulation has the same spatial distribution as a test beam being modulated, Eq. (7) can be multiplied by  $f(\mathbf{x})$  and integrated over the transverse coordinates  $\mathbf{x}$  to yield the total modulation at a given  $\theta$ . The result is

$$\langle \eta(\theta) \rangle = -a \frac{e^{i\theta} (k_u z - \theta)}{\sqrt{i\theta + 2\hat{\sigma}_x^2} \sqrt{i\theta + 2\hat{\sigma}_y^2}} + \text{c.c.}, \quad (8)$$

when  $0 \leq \theta \leq k_u z$ , and  $\eta(\theta) = 0$  otherwise. Eq. (8) can be compared to the longitudinal phase space measured in the TCAV when the transverse beam size is different in  $x$  and  $y$ . If  $\hat{\sigma}_y = \hat{\sigma}_x = \hat{\sigma} = \sqrt{k k_u} \sigma$ , some manipulation yields

$$\langle \eta(\theta) \rangle = -2a (k_u z - \theta) \frac{2\hat{\sigma}^2 \cos \theta + \theta \sin \theta}{\theta^2 + 4\hat{\sigma}^4} \quad (9)$$

when  $0 \leq \theta \leq k_u z$ , and  $\eta(\theta) = 0$  otherwise. Evidently the beam size plays an important role in governing the amplitude and phase of modulation.

What we have described thus far is the effect of a Gaussian pancake electron beam emitting a diffracting photon beam that modulates test electrons in front of it. The diffracting beam is born with an rms waist size of  $\sigma$ , so it is natural to identify the Rayleigh range

$$z_R = \frac{1}{2} k \sigma^2 = \frac{1}{2k_u} \hat{\sigma}^2. \quad (10)$$

When  $\theta \gg 2\hat{\sigma}^2 = 4k_u z_R$ , significant diffraction has occurred, and the modulation follows a  $\text{sinc}(\theta)$  behavior. On the other hand, when  $\theta \ll 4k_u z_R$ , no diffraction has occurred, and the modulation follows a  $\cos(\theta)$  pattern. The difference in phase between these regimes can be attributed to the Gouy phase shift. If one assumes a transverse beam size of  $100 \mu\text{m}$  and parameters given in Table 1,  $4k_u z_R$  is of order unity. This implies that the modulation near the source is strongly dependent upon the precise beam size.

The effect of beam size on the modulation amplitude is shown in Figure 2. For the parameters relevant to our experiment, beam sizes in excess of  $200 \mu\text{m}$  severely limit the chirp on the first portion of the beam that can be compressed.

The modulation described here can be convolved with a current profile to approximate the modulation expected from a real electron beam. We leave this discussion for another forum. Other figures of merit, like the induced energy spread, could also be calculated.

Table 1: Wiggler and Beam Parameters

Parameter	Value
wiggler K value	40
wiggler length (cm)	180
wiggler period (cm)	30
beam energy (GeV)	3.32
resonant wavelength ( $\mu\text{m}$ )	2.84
tail charge (pC)	50
beam size ( $\mu\text{m}$ )	variable

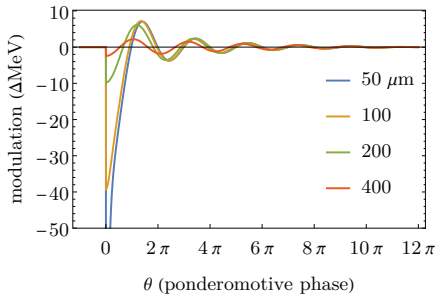


Figure 2: The modulation amplitude plotted as a function of the transverse rms beam size. In this diagram a 50 pC pancake beam sitting at  $\theta = 0$  modulates a test beam at  $\theta > 0$  over 6 wiggler periods.

## 1D LIÉNARD–WIECHERT MODEL

The single frequency FEL approach of the previous section is useful for estimating the importance of diffraction. However, violation of the slowly varying envelope approximation leads to questionable modulation behavior near the source. Unfortunately this is where the modulation is the largest.

Another way to approach this problem is by directly computing the Liénard–Wiechert field from the source, and integrating over the sustained interaction. E. Saldin [7] did this for a 1D beam traveling in an infinite planar wiggler, and J. Wu [8] simplified his expression for  $K \gg 1$ .

The result from E. Saldin’s work is an expression for the energy loss rate  $d\mathcal{E}/dt$  of a 1D snake-like beam,

$$\frac{d\mathcal{E}}{cdt} = e^2 k_u \int_{-\infty}^s ds' D(\hat{s} - \hat{s}', K, \hat{z}) \frac{d\lambda(s')}{ds'}, \quad (11)$$

where  $D$  is a function that can be calculated, and  $\lambda(s)$  is the linear bunch density, and  $s$  is the longitudinal coordinate along the bunch. J. Wu averaged  $D$  along a single wiggler period for  $K \gg 1$ . A cartoon of the physical picture is given in Figure 3.

This model should give accurate results when the sinusoidal oscillation amplitude is much larger than the transverse beam size,

$$\frac{K}{k_u \gamma} \gg \sigma. \quad (12)$$

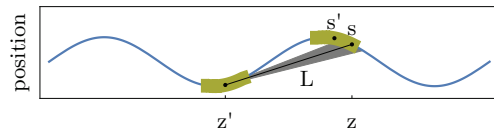


Figure 3: The energy modulation at bunch coordinate  $s$  is calculated by finding the field from bunch coordinate  $s'$  at the retarded position  $z'$ , and then integrating over all  $s'$ .

For the parameters of Table 1,  $K/k_u \gamma \approx 300 \mu\text{m}$ , and we expect a beam size of order  $100 \mu\text{m}$  or less in both dimensions.

We skip right to the result, shown in Figure 4. In this graphic three Gaussian current profiles of variable rms width (dashed) produce an energy modulation (solid) that is roughly sinusoidal, with a large enhancement near  $\theta = 0$ . Wiggler and beam parameters are given in Table 1.

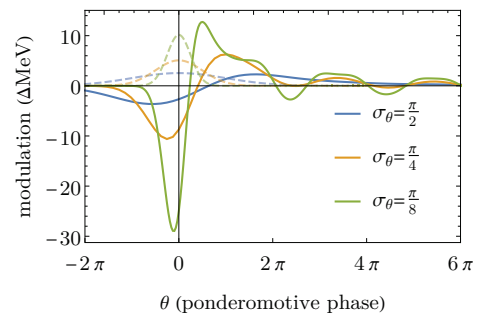


Figure 4: The energy modulation (solid) resulting from a 1D beam with a variable rms duration. The current in arbitrary units is shown in a matching color scheme (dashed).

In the case of  $\sigma_\theta = \pi/2$ , the beam is too wide to radiate with a single phase, and the modulation suffers. When the charge is kept constant and the pulse shortened to  $\sigma_\theta = \pi/8$ , a decaying sinusoidal modulation with harmonic content is predicted.

## CONCLUSION

We have gained some insight into the transverse beam size dependence of the modulation from the FEL model, and some insight into the longitudinal beam size dependence from the CSR model. Neither model is optimal for our problem, and we are actively investigating alternatives. A 3D CSR model, incorporating both the transverse beam size and current profile, would be preferable.

## REFERENCES

- [1] S. Zholents, “Method of an enhanced self-amplified spontaneous emission for x-ray free electron lasers,” *Phys. Rev. ST Accel. Beams*, vol. 8, p. 040701, Apr. 2005.
- [2] P. Emma, “Attosecond x-ray pulses in the LCLS using the slotted foil method,” *Phys. Rev. ST Accel. Beams*, SLAC-PUB-10712, 2004.
- [3] A. Lutman, “Fresh-slice multicolour X-ray free-electron lasers,” *Nat. Photonics*, vol. 10, p. 745, Oct. 2016.

- [4] M. Guetg, "Generation of High-Power High-Intensity Short X-Ray Free-Electron-Laser Pulses," *Phys. Rev. Lett.*, vol. 120, p. 014801, Jan. 2016.
- [5] Z. Huang, "Measurements of the linac coherent light source laser heater and its impact on the x-ray free-electron laser performance," *Phys. Rev. ST Accel. Beams*, vol. 13, p. 020703, Feb. 2010.
- [6] K. Kim, Z. Huang, and R. Lindberg, *Synchrotron Radiation and Free-Electron Lasers: Principles of Coherent X-Ray Generation*, Cambridge University Press, 2017.
- [7] E. Saldin *et al.*, "Radiative interaction of electrons in a bunch moving in an undulator," *Nucl. Instrum. Methods Phys. Res.*, vol. 18, p. 158, Nov. 1998.
- [8] J. Wu *et al.*, "Calculation of the coherent synchrotron radiation impedance from a wiggler," *Phys. Rev. ST Accel. Beams*, vol. 6, p. 040701, Apr. 2003.